CHEMISTRY
AN ASIAN JOURNAL
www.chemasianj.org

## Accepted Article

**Title:** Ambidextrous α,γ-Hybrid Peptide Foldamers

**Authors:** Rajkumar Misra, Gijo George, Abhijith Saseendran, Srinivasarao Raghothama, and Hosahudya Gopi



**To be cited as:** *Chem. Asian J.* 10.1002/asia.201901411

**Link to VoR:** http://dx.doi.org/10.1002/asia.201901411

A Journal of
ACES Asian Chemical Editorial Society

A sister journal of Angewandte Chemie and Chemistry – A European Journal

WILEY-VCH

10.1002/asia.201901411

# Ambidextrous α,γ-Hybrid Peptide Foldamers

Rajkumar Misra,[a] Gijo George,[b] Abhijith Saseendran,[a] Srinivasarao Raghothama,[b] Hosahudya N. Gopi[a]*

[a]Department of Chemistry, Indian Institute of Science Education and Research, Dr. Homi Bhabha Road, Pashan, Pune-411 008, E-mail: hn.gopi@iiserpune.ac.in

[b]NMR Research Center, Indian Institute of Science, Bangalore-560012, India

**ABSTRACT:** Molecular chirality is ubiquitous in nature. The natural biopolymers, proteins and DNA, preferred right-handed helical bias due to the inherent stereochemistry of monomer building blocks. Here, we are reporting a rare co-existence of left and right-handed helical conformations and helix terminating property at the C-terminus within a single molecule of α,γ-hybrid peptide foldamers composed of achiral Aib (α-aminoisobutyric acid) and 3,3-dimethyl substituted γ-amino acid (Adb; 4-amino-3,3-dimethylbutanoic acid). The molecular level left- and right-handed helical screw sense of α,γ-hybrid peptides are representing a macroscopic tendril perversion. The pronounced helix terminating behaviour of C-terminal Adb residues was further explored to design helix-Schellman loop mimetics and to study their conformations in solution and single crystals. The stereochemical constraints of dialkyl substitutions on γ-amino acids have showed a marked impact on the folding behaviour of α,γ-hybrid peptides.

10.1002/asia.201901411

## INTRODUCTION

Helicity is the most common structural feature associated with many kinds of molecules including biopolymers.[1] As proteins are exclusively built from L-amino acids, this stereochemical bias is reflected in their strong preference to right-handed (*P*) helices over the left-handed (*M*) helices. Nevertheless, a recent systematic survey of protein crystal structures revealed the presence of short left-handed helices.[2] Along with helices from chiral amino acids, significant efforts have been made in the literature to build helices completely from achiral amino acids such as Aib and its higher dialkyl substituted analogs.[3,4] Due to their intrinsic conformational restriction, Aib residues invariably promote helical conformations. This helix nucleating property of Aib has been widely explored to design α- and $3_{10}$-helices. The helices constructed entirely from achiral Aib residues have shown to adopt both (*P)*-and (*M*)-helices. These two helices are topologically equivalent enantiomers.

Compared to the limited set of α-peptide helices, foldamers composed of unnatural β- and γ-peptides uncovered various helical types with distinct intramolecular H-bonding pattern.[5,6] Instructively, majority of β- and γ-peptides foldamers showed H-bonding between 1→4 residues, similar to the $3_{10}$-helices. Moreover, foldamers composed of complete achiral β- and γ-amino acids have not been scrutinized as those of corresponding chiral amino acids. Nonetheless, Seebach and colleagues demonstrated a stair-like 8-helices[7] and uncommon extended sheets from the oligomers of α,α-dialkyl β-amino acids.[8] In continuation, Balaram and colleagues showed 9-helical(1→3, H-bonds) conformations from the oligomers of achiral 3,3-dialkyl substituted γ-amino acid gabapentin (gpn),[9] and 12- helices (1→4, H-bonds) from achiral hybrid peptides composed of Aib and gabapentin.[10]

10.1002/asia.201901411

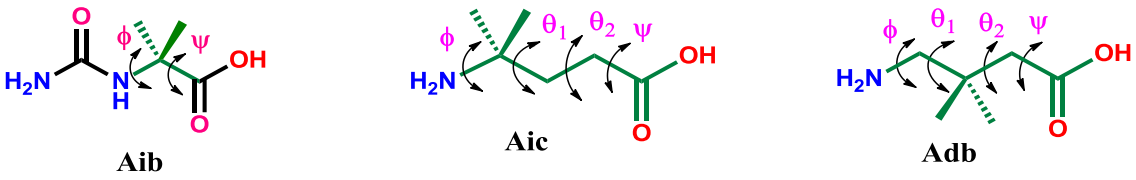


**Figure 1**. Chemical structure of Aib (α-aminoisobutyric acid), Aic (4-aminoisocaproic acid, doubly homologated Aib) and Adb (4-amino-3,3-dimethylbutanoic acid, present study).

In a sharp contrast to the $3_{10}$-helices of Aib oligomers, the double homologated Aib (4,4-dimethyl substituted γ-amino acid, Aic, Figure 1) oligomers have shown to adopt extended sheet type conformations and to spontaneously self-aggregates into fibers.[11] Additionally, the combination of Aic with helix inducing Aib in 1:1 alternating α,γ-hybrid peptides showed the co-existence of 15/17- helices (1→5 H-bonds) and 12-helices(1→4 H-bonds) in single crystals,[12] analogous to the α- helix (1→5 H-bonds) and $3_{10}$-helices(1→4 H-bonds) of α-peptides.

These remarkable structural features of hybrid peptides composed of 4,4-dimethyl γ-amino acid, motivated us to examine the impact of dimethyl substitutions at the β-position on γ-residues (4-amino-3,3-dimethyl butanoic acid, Adb, Figure 1) and their folding behavior in α,γ-hybrid peptides. Herein, we are reporting a rare co-existence of left- and right- handed helical screw sense and a remarkable helix terminating property at the C-terminus within a single molecule of achiral α,γ-hybrid peptide foldamers composed of 1:1 alternating Aib and Adb residues. The pronounced helix terminating behavior was further explored to design Schellman loop mimetics.

10.1002/asia.201901411

## RESULTS AND DISCUSSION

The sequences of achiral α,γ-hybrid peptides (**P1-P4**) under investigation are shown Scheme 1.

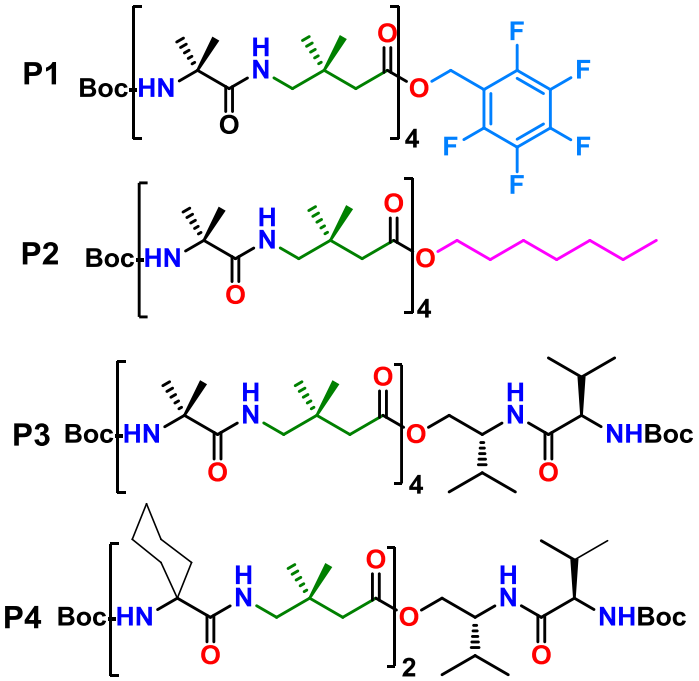


**Scheme 1:** Sequences of α,γ-hybrid peptides

The 3,3-dimethyl γ-amino acid was synthesized in excellent yield through the Michel addition of nitromethane[13] to 2,2-dimethyl ethyl acrylate, and subsequent transformation of nitro into amine by catalytic hydrogenation. The schematic representation of the 3, 3-dimethyl γ-amino acid synthesis is shown in Scheme 2.

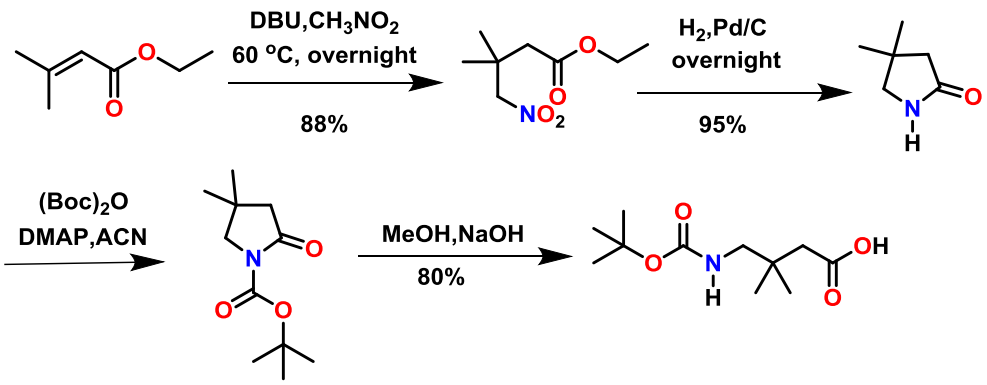


**Scheme 2:** Synthesis of *N*-Boc protected 3,3-dimethylbutanoic acid (Adb):

10.1002/asia.201901411

All hybrid peptides were synthesized by solution phase chemistry using EDC/HOBt as coupling agents and purified through reverse phase HPLC.

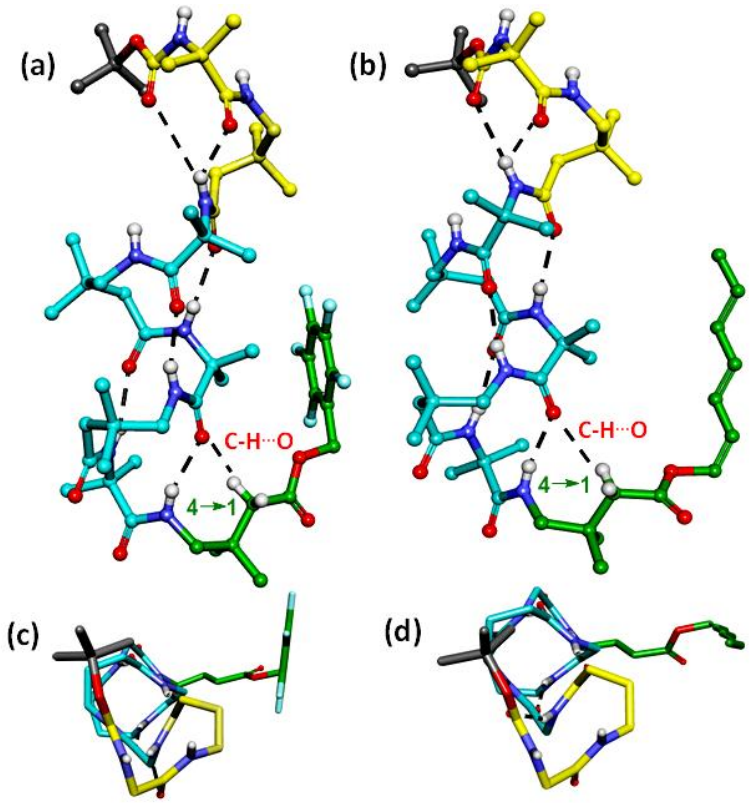


**Figure 2**: X-ray structure of peptides (a) **P1** and (b) **P2**. The left- and right-handed helical conformations are highlighted in yellow and cyan, respectively. The helix terminating C-terminal Adb esters are highlighted in green. Top view of **P1** and **P2** are shown in (c) and (d), respectively. The top views provide a clear distinction of left and right handed helical conformations.

Initially, the octapeptide **P1** was designed to understand whether this peptide can adopt 12- or 15/17- helix similar to its Aib/Aic analogues.[12] As crystal structures provide an useful information on the folding properties of hybrid peptides, we attempted to grow X-ray quality crystals of **P1** in various solvent combinations. To facilitate the crystallization, we used pentafluorobenzyl ester of Adb at the C-terminus. Single crystals of **P1** obtained in aqueous

10.1002/asia.201901411

MeOH solution yielded an interesting structure shown in Figure 2a. The local conformation of Adb residues is described by the backbone torsion angles $\phi$(N-C$^{\gamma}$), $\theta_1$(C$^{\gamma}$-C$^{\beta}$), $\theta_2$(C$^{\beta}$-C$^{\alpha}$) and $\psi$(C$^{\alpha}$-C=O). The torsion angles of Adb residues are given in the Table 1. Notably, **P1** adopted an uncommon helix conformation with the co-existence of left- and right-handed helical screw sense, along with a remarkable reversal of helix directionality at the C-terminus. Being an achiral system, two molecules with opposite handedness are present in the asymmetric unit. The structure adopted by the peptide **P1** representing a phenomenon observed in macroscopic "tendril perversion".[14] This type of opposite screw sense is a subject of interest, and the co-existence of left- and right-handed helical screw sense is rather unusual in peptide foldamers. Recently, Clayden and colleagues have demonstrated the tendril perversion at molecular level by introducing amino acids opposite chirality at the *N*- and *C*-terminus of a helix composed of achiralAib oligomers.[15] The crystal structure analysis of **P1** reveals three interesting features; the two *N*-terminus residues adopted a left-handed helix screw sense, while the middle five residues adopted a right-handed helix screw sense, and finally the C-terminal Adb ester adopted a left-handed conformation with reversal helix directionality. The hydrogen bond parameters of **P1** are tabulated in the Table S2. The *N*-terminus left-handed helix is stabilized by a weak 12-membered H-bond between Boc CO and Aib3NH ($i \rightarrow i+3$) as well as a nine membered H-bond between the Aib 1CO andAib3 NH ($i \rightarrow i+2$).

**Table 1: Torsion angles of Adb residues in the hybrid peptides P1, P2 and P4**

| Peptide | Residue | $\phi$ ° | $\theta_1$ ° | $\theta_2$ ° | $\psi$ ° |
|---|---|---|---|---|---|
| **P1** | Adb(2)[a] | 114 | -56 | -76 | 90 |
| | Adb(4) | -126 | 57 | 55 | -111 |
| | Adb(6) | -126 | 52 | 63 | -112 |
| | Adb(8)[b] | 99 | 59 | 176 | 169 |
| **P2** | Adb(2)[a] | 125 | -56 | -66 | 97 |

| | | | | | |
|---|---|---|---|---|---|
| | Adb(4) | -125 | 59 | 55 | -115 |
| | Adb(6) | -133 | 54 | 59 | -106 |
| | Adb(8)[b] | 106 | 65 | 177 | 109 |
| **P4** | Adb[a] | 126 | -56 | -62 | 120 |
| | Adb[b] | -106 | 63 | 80 | -42 |

[a]Residues are part of left-handed helices. [b]Residues are not part of a helix.

Interestingly, Adb4 NH is not participating in the canonical H-bonding, and this type of non H-bonding partners have been observed at the junction of left- and right-handed helical fusion.[15,16] The right-handed helix observed from the residues Aib3 to Aib7 is stabilized by 12-membered H-bonds (12-helix) between the residues *i* and *i+3*, which is the most stable helix conformation observed in the α,γ-hybrid peptides composed of $\gamma^4$-amino acids.[17] In contrast to the *gauche (g)* and *extended (t)* conformations along $C^{\gamma}$-$C^{\beta}$ and $C^{\beta}$-$C^{\alpha}$ bonds adopted by the Aic residues in a 12-helix,[12] the Adb residues have adopted *g, g* conformations similar to $\gamma^4$-residues.[16] The C-terminal Adb ester adopted a left-handed helix conformation with reversal of helix direction. Instructively, the torsion variables $\theta_2$ and ψ ($C^{\beta}$-$C^{\alpha}$-C(O)'-O] adopted extended conformation. In addition, the C-terminal twist is stabilized by a 15 membered C-H···O H-bond between Aib6 CO and $C^{\alpha}$H of Adb8 [C-**H**···**O** dist. 2.43Å and ∠ C-H···O is 125°]. The C-terminal helix reversal of **P1** is representing a Schellman motif observed in protein structures.[18] Schellman noted that helices in proteins are often terminated at the C-terminal residue by adopting a left-handed conformation. It is pertinent to note that the helix terminating residue is invariably achiral Gly and less frequently Asn. Similar type of helix termination is often observed in synthetic α-peptide helices containing C-terminal Aib esters.[19] We speculated that the C-H···O H-bond observed at the C-terminus of **P1** and the

intermolecular head-to-tail H-bonds between the helices in the crystalpacking may be responsible for the helix termination.[18f]

The unusual left- and right-handed helical screw sense along with the Schellman motif type helix reversal motivated us to design peptide **P2** and examine whether the observed structure is unique to **P1** or it can persist across other α, γ-hybrid peptides of achiral Aib and Adb. In **P2**, we chose to incorporate n-heptanol ester of Adb to assess if the helix reversal is not due to the aromatic π-staking as well as to verify whether the n-alkane can also fold back towards the helix. Single crystals of **P2** grown in aqueous methanol solution yielded the structure shown in Figure 2b. Similar to **P1**, **P2** adopted a rare helical conformation associated with left- and right-handed helix screw sense. The first two residues adopted the left-handed helix conformation, stabilized by a weak 12-membered H-bond between Boc CO and Aib3 NH and a strong nine membered H-bond between Aib 1 CO and Aib3 NH. As observed earlier, Adb4NH is not participating in the canonical intramolecular H-bonding. The H-bond parameters are tabulated in the Table S4 (See ESI). Residues from Aib3 to Aib7 adopted a right-handed 12-helix conformation with similar torsion variables as observed in **P1** (Table 1). As anticipated, the C-terminal Adb ester displayed a Schellman motif type helix terminating property. Interestingly, the n-heptane chain fold back towards *N*-terminus of the helix. In addition, the C-terminal helix reversal is stabilized by a 15 membered C-H···O H-bond between Aib6 CO and $C^{\alpha}H$ of Adb8 [C-H···O dist. 2.49 Å and ∠C-H···O is 149°]. The conformational analysis of n-heptanol ester reveals that C-C bonds with the exception of C1-C2, other assumed antiperiplanar conformation. The C1-C2 and ester C-O bonds adopted *gauche* and *anticlinal* conformations, respectively.

Inspired by the co-existence of opposite helix screw sense and helix terminating property, we sought to investigate whether this property can be explored to design Schellman loops. The helix-Schellman loop-helix structures are often found in proteins.[18] We hypothesize

10.1002/asia.201901411

that instead of alkyl or aryl esters, if the C-terminal Adb is esterified with peptide alcohols it may be possible to design Schellman loops. In this context, peptide **P3** was designed (Scheme 1). We chose Boc-Val-Val-ol (dipeptide alcohol) for the C-terminal esterification. As peptide **P3** did not yield X-ray quality single crystals, we subjected the peptide to 2D NMR analysis in $CDCl_3$ at room temperature (298K). The analysis of ROESY spectrum of **P3** revealed strong NH↔NH NOEs between Aib1↔Adb2, Aib5↔Adb6, Aib7↔Adb8 and Val9↔Val10, and weak NH↔NH NOEs between Aib2↔Adb3 and Adb4↔Aib5. In addition, medium NOEs between Aib3NH↔$C^{\gamma}$HAdb2, Aib5NH↔$C^{\gamma}$HAdb4, Aib7NH↔$C^{\gamma}$HAdb6, and strong Aib3NH↔$C^{\alpha}$HAdb2, Aib5NH↔$C^{\alpha}$HAdb4, Aib7NH↔$C^{\gamma}$HAdb6, and Val9NH↔$C^{\alpha}$H Val10, and a weak NOE between Val9NH↔$C^{\gamma}$HAdb8 were also observed. Further, the DMSO titration studies suggested that except the *N*-terminusAib1 and Adb 2 NHs, no pronounced chemical shift variation is observed in other amideNHs. It is fairly surprising that the amide NHs of Val-Val residues are also not exposed to solvent, indicating their involvement in the intramolecular H-bonding. Using unambiguous NH↔NH and other NOEs, the solution structure of **P3** was generated and the superposition of ten lowest energy minimized structures is shown in Figure 3. Instructively, the peptide adopted a continuous right-handed 12-helix conformation up to Aib7. The C-terminal Adb adopted a left-handed helical conformation. Intriguingly, the Val9 and Val10 NHs are involved in the bifurcated H-bonds with Aib7CO. The average torsion values of NMR derived structures are given in the Table S8. Overall, the structure of **P3** resembling a helix-Schellman loop conformation observed in the protein structures.[17]

10.1002/asia.201901411

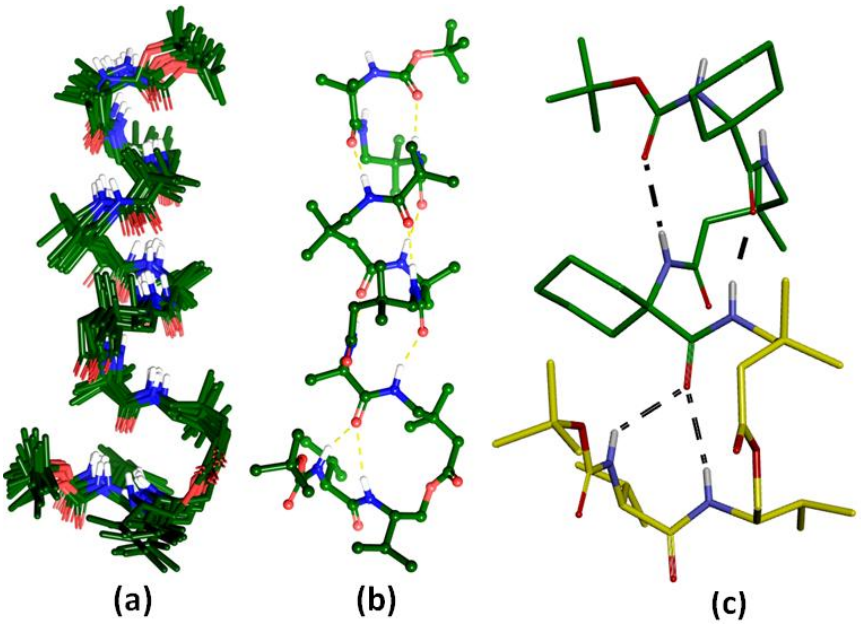


**Figure 3**: Solution NMR structures of peptide **P3** (a) and (b), and X-ray structure of **P4** (c).

To realize the helix-Schellman loop type conformation of α,γ-hybrid peptides in single crystals and to support the solution structure of **P3**, we synthesized several α,γ-hybrid peptides from hexa to octapeptides composed of achiral amino acids with Boc-Val-Val-ol ester of C-terminal Adb. Among all the peptides synthesized, the hexapeptide **P4** (Scheme 1) composed of alternating $Ac_6c$ (1-aminocyclohexane-1-carboxylic acid) and Adb yielded X-ray quality crystals in aprotic $CHCl_3$. The X-ray structure of **P4** is shown in Figure 3c. The first three residues of **P4** adopted a right handed 12-helix conformation, while the C-terminal Adb4 adopted a left-handed helical conformation. The torsion angles of Adb residues are given in the Table 1. Structural analyses revealed that the C-terminus Boc-Val-Val dipeptide ester adopted a semi-extended type conformation. Notably, the carbonyl of $Ac_6c3$ is participated in three-center H-bonds with amide NHs of Val5 (2→4) and Val6 (1→4) involving 12 and 15 membered pseudocycles, respectively. Interestingly, the concavity induced at the site of bifurcated H-bonds is occupied by the solvent $CHCl_3$. The crystal structure of **P4** is mimicking helix-Schellman loops in protein structures, and in complete agreement with the solution structure

of **P3**. Moreover, the helix terminating property of Adb esters is found to be persistent across the Aib/Adb hybrid peptide foldamers.

## CONCLUSION

In summary, we have demonstrated the unique folding properties of achiral α,γ-hybrid peptides composed of Aib and Adb. The two octapeptides (**P1** and **P2**) have shown to adopt helical conformations with opposite chirality, along with the helix terminating property at the C-terminal Adb esters. Accommodation of three different structural features in a single peptide foldamer is unprecedented. The Schellman motif type helix reversal is consistent across the hybrid peptides studied. The stabilization of the Val-Val dipeptide through three center H-bonds resembling the Schellman loops in protein structures. The study further reveals that the position of dialkyl substitutions on γ-amino acids has a major impact on the folding properties of γ-peptide foldamers and also induces fragility into the 12-helix conformations of α,γ-hybrid peptides. More importantly, the role of protic solvents in the induction of opposite chirality within the helix cannot be ruled out. Overall, the simple chemistry of amino acid synthesis and the unique structural properties of α,γ-hybrid peptides presented here can be further explored to design novel foldamers.

## EXPERIMENTAL SECTION

All amino acids, ethyl 3,3-dimethylacrylate,nitro methane, Pd/C, TFA, EDC, HOBt, DIEPA, were commercially available. DCM, DMF, ethyl acetate and pet-ether (60-80 °C) were distilled prior to use. Column chromatography was performed on silica gel (120-200 mesh).Final peptides were purified on reverse phase HPLC (C18 column, MeOH/$H_2O$ 70:30-95:5 as gradient with flow rate 2.5 mL/min). $^1$H NMR and $^{13}$CNMR spectra were recorded on 400 MHz and on 100 MHz respectively, using residual solvent signal as internal standards ($CDCl_3$). Chemical shifts ($\delta$) reported in parts per million (*ppm*) and coupling constants (*J*) reported in

Hz. Mass spectra were recorded using MALDITOF/TOF and HRMS Electron Spray Ionization (ESI).

**NMR spectroscopy:** All NMR studies were carried out by using either 400 or 600 MHz spectrometer. Resonance assignments were obtained by TOCSY and ROESY analysis. All two-dimensional data were collected in phase-sensitive mode by using the time-proportional phase incrementation (TPPI) method. Sets of 1024 and 512 data points were used in the t2 and t1 dimensions, respectively. For TOCSY and ROESY analysis, 32 and 72 transients were collected, respectively. A spectral width of 6007 Hz was used in both dimensions. A spin-lock time of 200 and 250 ms were used to obtain ROESY spectra. Zero-filling was carried out to finally yield a data set of 2 K × 1 K. A shifted square-sine-bell window was used before processing.

**Molecular Dynamics (MD):** Structure calculation was done using a simulated annealing protocol in vacuum using DESMOND and OPLS 2005 force field with NOE and dihedral constraints. A fully extended peptide molecule (all backbone dihedral angles were kept to be 180˚) was kept in orthorhombic simulation cell of dimensions 40.96*66.43*32.40 Å. Upper limit for distance was kept at 3 Å and 4 Å for strong and medium NOEs. All the lower distance limits were taken to be 1.8 Å. 1 Kcal/Mol force constant was used for all the constraints. NOE potentials (appropriate for treating ambiguous NOE assignments) used are having the following form,

$E_{NOE}$ = **fc*** (**lower** - *d*)$^2$, if *d* <**lower**;

$E_{NOE}$ = 0, if **lower** <= *d* <= **upper**;

$E_{NOE}$ = **fc*** (**upper** - *d*)$^2$, if **upper** <*d* <= **upper** + **sigma**;

$E_{NOE}$ = **fc*** (a + **beta** * (*d* - **upper**) + c / (*d* - **upper**)), if *d* >**upper** + **sigma**;

where *d* is the distance and fc is the force constant.

Values of sigma and beta used in the calculation are 0.5 and 1.5 respectively. The values a and c are determined automatically such that potential is continuous and differential everywhere. Before production run simulation, a default NVT relaxation was done as implemented in DESMOND. NVT ensemble was used for the production run simulation. Berendsen thermostat with a relaxation time of 1 ps was used. A RESPA integrator was used in which for all the bonded interactions and near non-bonded interactions a time step of 1 fs was used and far non-bonded interaction time step of 3 fs was used. A cut-off of 9 Å was used for short range electrostatic interactions. A smooth particle mesh ewald method was used for treating long range electrostatic interactions. Simulated annealing was done in 6 stages. First stage consist simulation for 30 ps at 10 K. In the second stage, temperature was linearly increased to 100 K till 100 ps. In the third stage, temperature was linearly increased to 300 K till 200 ps. In the fourth stage, temperature was linearly increased to 400 K till 300 ps. In the fifth stage, temperature was maintained at 400 k till 500 ps. In the sixth stage, temperature was linearly decreased to 300 K till 1000 ps and maintained at 300 k till 1200 ps. 20 minimum energy structures were taken from the trajectory between 1000 ps and 1200 ps. The lowest energy structure from the trajectory between 1000 ps and 1200 ps was taken and minimized using a steepest descent method using a convergence gradient threshold of 0.05 kcal/mol/Å.

**Synthesis of N-Boc protected3,3-dimethylbutanoic acid (Adb):**

Ethyl 3,3-dimethylacrylate (6.4 g, 50 mmol) was dissolved in neat nitro methane (13.5 ml, 250 mmol, 5 molequivalents) and 1,8-diazabicyclo[5.4.0]undec-7-ene (DBU, 11.2 mL, 75 mmol, 1.5 molequivalents) were added. The mixture was heated at 60 °C overnight, and the nitromethane was evaporated under reduced pressure. Ethyl acetate and 1MHCl were added to the resulting residue, and the organic phase was separated. The acidic aqueous layer was washed twice with ethyl acetate, the combined organic phase was dried over $Na_2SO_4$, and the solvent was evaporated under reduced pressure. The product, 3,3-dimethyl-4-nitro-butyric acid

ethyl ester was collected (7.56 g, 80 % yield) as colorless oil. The suspension of activated Pd/C (20% by weight) and 3,3-dimethyl-4-nitro-butyric acid ethyl ester (3.78 g, 20 mmol) in MeOH (40 mL) and acetic acid(5mL) was stirred at room temperature in the presence of hydrogen. After completion of the reaction (TLC, ~36 hrs), Pd/C was filtered through the bed of celite and the filtrate was evaporated to dryness under vacuum to get gummy 4,4-dimethyl-2-pyrrolidinone (2.14 g, 95 % yield) as oil. The amide NH group of 4,4-dimethyl-2-pyrrolidinone was further protected with Boc group and then hydrolyzed using NaOH (2.0 M) in MeOH to get final product *N*-Boc protected 3,3-dimethylbutanoic acid (3.21 g, 80 % yield in two step)

**Synthesis of peptides P1-P5:**

All peptides were synthesized through conventional solution phase methods using fragment condensation strategy. The Boc group was used for the *N*-terminal protection and the C-terminus was protected as a benzyl ester. Couplings were carried out using *N*-Ethyl-*N′*-(3-dimethylaminopropyl)carbodiimide hydrochloride (EDC) and 1-hydroxybenzotriazole (HOBt). The *N*-terminal protecting groups was removed with trifluoroacetic acid C-terminal benzyl group was deprotected by catalytic hydrogenation. The octapeptide acid(Aib-Adp)$_4$–COOH was further reacted with pentafluorobenzyl bromide and heptyl bromide in presence of potsiumcarbonate and DMF as solvent to obtain compound **P1**and **P2**. For compound **P3**(Aib-Adb)$_4$–COOH was reacted with Boc-Val-Valol in presence of DCC and DMAP. In case of **P4**, the tetrapeptide acid, Boc-(Ac$_6$c-Adb)$_2$-COOH was coupled with Boc-Val-Valol in presence of DCC and DMAP. Finally, all the peptides were purified by RP-HPLC using MeOH/$H_2O$ gradient system.

## Structural data of the compound1and peptides:

**Compound 1:**

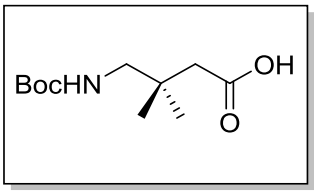


**$^1$H NMR** (400 MHz, DMSO-$d_6$) $\delta$ 11.94 (s, 1H), 6.86 – 6.55 (t, 1H), 2.86 (d, $J$ = 6.4 Hz, 2H), 2.06 (s, 2H), 1.37 (s, $J$ = 1.2 Hz, 9H), 0.89 (s, 6H). $^{13}$C NMR (101 MHz, DMSO) $\delta$ 173.53, 156.54, 77.89, 50.55, 44.05, 34.82, 28.70, 25.07. HR-MS m/z calculated value for $C_{11}H_{21}NO_4$ is $[M+Na]^+$ 254.1368 and observed 254.1370

**PeptideP1:**

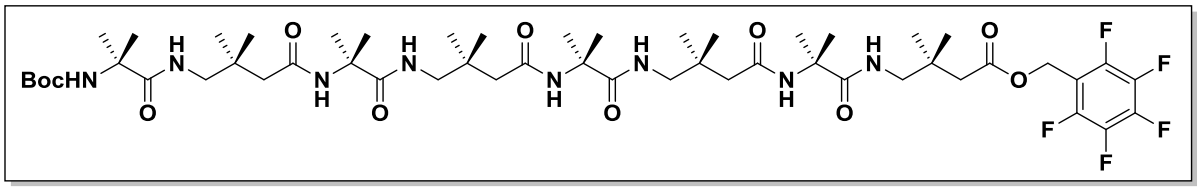


**$^1$HNMR** (600 MHz, Chloroform-*d*) $\delta$ 8.17 (s, 1H), 8.03 (s, 1H), 7.80 (t, $J$ = 6.5 Hz, 1H), 7.71 (s, 1H), 7.61 (t, $J$ = 6.5 Hz, 1H), 7.59 – 7.49 (m, 1H), 6.55 (t, $J$ = 6.2 Hz, 1H), 5.16 (s, 2H), 4.98 (s, 1H), 3.27 – 3.04 (m, 8H), 2.33 (s, 2H), 2.06 (d, $J$ = 11.3 Hz, 6H), 1.56 – 1.36 (m, 33H), 1.11 – 0.92 (m, 24H).$^{13}$C NMR (151 MHz, $CDCl_3$) $\delta$ 175.65, 175.38, 175.23, 171.50, 171.21, 171.17, 171.01, 154.99, 146.21, 144.56, 137.94, 136.33, 130.77, 128.58, 80.10, 77.37, 77.16, 76.95, 56.76, 56.48, 52.57, 49.30, 48.08, 47.61, 39.79, 38.17, 35.30, 35.17, 35.04, 29.40, 28.24, 26.83, 26.67, 26.53, 25.15, 24.99, 24.83.MALDITOF/TOF- *m/z*calcd.for$C_{52}H_{83}F_5N_8O_{11}$ $[M+Na]^+$ 1113.59, obsrvd. 1113.76

**PeptideP2:**

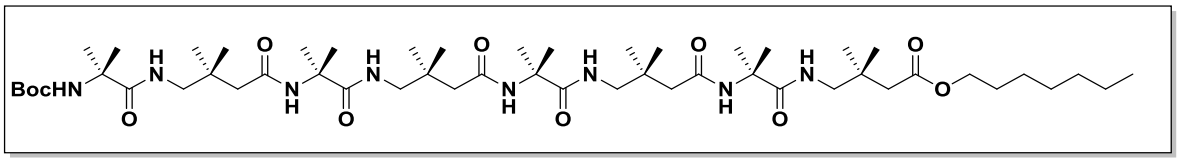


**$^1$HNMR** (400 MHz, Chloroform-*d*) $\delta$ 8.15 (s, 1H), 8.06 (s, 1H), 7.76 – 7.68 (m, 2H), 7.63 (t, $J$

10.1002/asia.201901411

= 6.5 Hz, 1H), 7.53 (d, *J* = 7.7 Hz, 1H), 6.59 (t, *J* = 6.1 Hz, 1H), 5.06 (s, 1H), 4.03 (t, *J* = 6.8 Hz, 2H), 3.25 – 3.08 (m, 8H), 2.28 (s, 2H), 2.11 – 2.00 (m, 6H), 1.69 (s, 5H), 1.50 – 1.43 (m, 27H), 1.35 – 1.21 (m, 9H), 1.04 (dd, *J* = 12.3, 6.5 Hz, 24H), 0.90 – 0.83 (m, 3H). $^{13}$C NMR (151 MHz, $CDCl_3$) δ 176.01, 175.64, 174.98, 172.83, 171.77, 171.49, 171.22, 155.15, 81.17, 77.37, 77.16, 76.95, 64.44, 57.46, 57.12, 57.01, 49.61, 48.60, 48.45, 47.98, 44.82, 44.67, 44.42, 35.54, 35.46, 35.35, 31.86, 29.05, 28.79, 28.51, 27.25, 27.01, 26.89, 26.07, 25.64, 25.54, 25.45, 22.71, 14.20.MALDITOF/TOF- *m/z*calcd.for$C_{52}H_{96}N_8O_{11}$ $[M+Na]^+$ 1031.70, obsrvd. 1031.85.

**Peptide P3:**

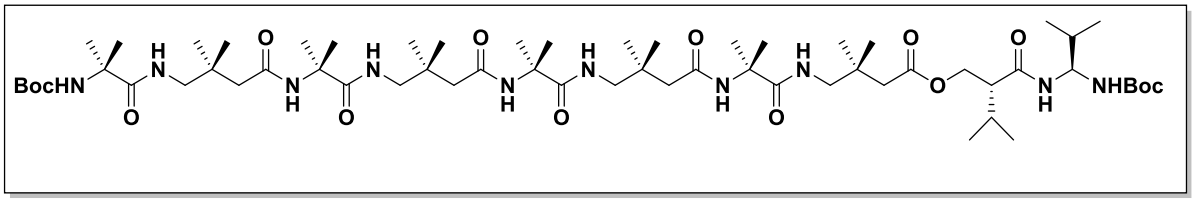


**$^1$H NMR** (600 MHz, Chloroform-*d*) *δ* 8.21 (d, *J* = 9.8 Hz, 2H), 7.90 (t, *J* = 6.5 Hz, 1H), 7.75 (s, 1H), 7.70 (t, *J* = 6.6 Hz, 1H), 7.59 (s, 1H), 7.54 (d, *J* = 9.3 Hz, 1H), 6.59 (t, *J* = 6.4 Hz, 1H), 5.53 (d, *J* = 9.2 Hz, 1H), 5.06 (d, *J* = 15.7 Hz, 1H), 4.19 (d, *J* = 2.8 Hz, 2H), 4.03 – 3.96 (m, 1H), 3.90 (tt, *J* = 9.2, 3.2 Hz, 1H), 3.29 – 3.09 (m, 10H), 2.15 – 2.05 (m, 9H), 1.57 – 1.41 (m, 57H), 1.11 – 0.99 (m, 32H), 0.98 – 0.90 (m, 15H).$^{13}$C NMR (151 MHz, $CDCl_3$) *δ* 175.98, 175.71, 175.42, 174.69, 172.14, 171.91, 171.87, 171.34, 171.05, 155.84, 154.98, 81.19, 79.13, 64.11, 60.23, 57.38, 56.99, 56.86, 53.80, 48.37, 48.28, 47.80, 44.68, 44.46, 44.28, 43.29, 35.37, 35.35, 35.24, 34.98, 31.31, 30.94, 28.98, 28.36, 27.11, 26.98, 26.88, 26.73, 26.30, 25.96, 25.59, 25.48, 25.35, 25.12, 19.65, 19.53, 17.97.MALDITOF/TOF- *m/z*calcd.for$C_{60}H_{110}N_{10}O_{14}$ $[M+Na]^+$1217.81, obsrvd. 1217.99

**Peptide P4:**

10.1002/asia.201901411

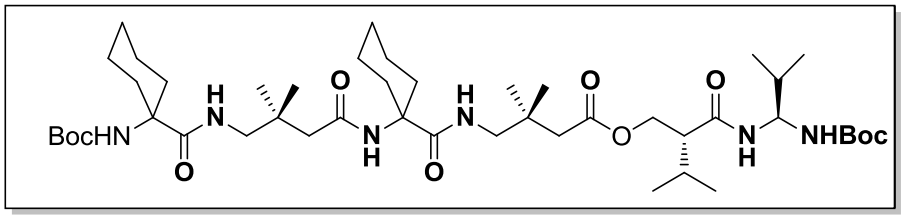


**$^1$H NMR** (400 MHz, Chloroform-*d*) $\delta$ 7.68 (s, 1H), 7.49 (d, *J* = 9.0 Hz, 2H), 6.87 (d, *J* = 7.7 Hz, 1H), 5.38 (d, *J* = 9.2 Hz, 1H), 4.87 (s, 1H), 4.25 (d, *J* = 10.7 Hz, 1H), 4.11 (d, *J* = 7.4 Hz, 1H), 3.98 (t, *J* = 8.2 Hz, 1H), 3.87 (td, *J* = 9.2, 4.8 Hz, 1H), 3.54 – 3.41 (m, 1H), 3.27 – 3.06 (m, 2H), 3.01 (d, *J* = 14.2 Hz, 1H), 2.30 (dd, *J* = 31.5, 14.5 Hz, 2H), 2.20 – 2.00 (m, 4H), 1.99 – 1.72 (m, 9H), 1.72 – 1.54 (m, 7H), 1.50 – 1.20 (m, 22H), 1.11 – 0.84 (m, 25H).$^{13}$C NMR (126 MHz, $CDCl_3$) $\delta$ 175.54, 175.37, 172.01, 156.97, 155.97, 154.89, 80.67, 79.41, 77.41, 77.16, 76.91, 64.15, 60.46, 60.28, 59.54, 53.86, 49.36, 48.32, 48.09, 45.05, 43.36, 35.40, 35.07, 34.07, 32.76, 32.35, 31.92, 31.70, 31.42, 29.82, 29.29, 28.50, 26.83, 26.61, 25.76, 25.51, 25.22, 25.08, 21.77, 21.45, 19.68, 19.53, 18.32.MALDITOF/TOF- *m/z*calcd.for$C_{46}H_{82}N_6O_{10}$ $[M+Na]^+$901.75, obsrvd. 901.75

**Crystallographic Information of Peptides:**

**Crystal structure analysis of (P1):** Crystals of peptide were grown by slow evaporation from a solution of aqueous methanol. A single crystal (0.24 × 0.09 × 0.12 mm) was mounted on loop with a small amount of the paraffin oil. The X-ray data were collected at 100K temperature on a Bruker APEX(II) DUO CCD diffractometer using Mo $K_\alpha$ radiation ($\lambda$ = 0.71073 Å), $\omega$-scans ($2\theta$ = 56.804), for a total of 15327 independent reflections. Space group P-1, a = 12.4211(17), b = 14.978(2), c = 18.010(2), $\alpha$ = 86.938(3),$\beta$ = 72.999(3),$\gamma$ = 73.465(3),V = 3070.1(7)Å$^3$, triclinic, Z = 2 for chemical formula $C_{53}$ $H_{86}$ $F_5$ $N_8$ $O_{12}$, with one molecule in asymmetric unit; $\rho$calcd = 1.214 gcm$^{-3}$, $\mu$ = 0.096 mm$^{-1}$, F(000) = 1280, The structure was obtained by direct methods using SHELXS-97.[1] The final R value was 0.0611 (wR2 = 0.1421) 4923 observed

reflections ($F_0 \geq 4\sigma(|F_0|)$) and 558 variables, S = 0.895.The largest difference peak and hole were 0.474 and -0.506eÅ$^3$, respectively

**Crystal structure analysis of (P2):** Crystals of peptide were grown by slow evaporation from a solution of aqueous methanol. A single crystal (0.34 × 0.06 × 0.18 mm) was mounted on loop with a small amount of the paraffin oil. The X-ray data were collected at 100K temperature on a Bruker APEX(II) DUO CCD diffractometer using Mo $K_\alpha$ radiation (λ = 0.71073 Å), $\omega$-scans ($2\theta$ = 57.728), for a total of 16084 independent reflections. Space group P-1, a = 13.932(10), b = 14.137(10), c = 17.651(14), $\alpha$ = 103.854(18),$\beta$ =100.946(19),$\gamma$= 108.442(17),V = 3066(4)Å$^3$, triclinic, Z = 2 for chemical formula $C_{53}$ $H_{93}$ $N_8$ $O_{12}$, with one molecule in asymmetric unit; $\rho$calcd = 1.120 gcm$^{-3}$, $\mu$ = 0.079 mm$^{-1}$, F(000) = 1342, The structure was obtained by direct methods using SHELXS-97.[1] The final R value was 0.1173 (wR2 = 0.0.2192) 5639 observed reflections ($F_0 \geq 4\sigma(|F_0|)$) and 679 variables, S = 1.128.The largest difference peak and hole were 0.295 and -0.445 Å$^3$, respectively

**Crystal structure analysis of (P4):** Crystals of peptide were grown by slow evaporation from a solution of chloroform. A single crystal (0.31 × 0.04 × 0.20 mm) was mounted on loop with a small amount of the paraffin oil. The X-ray data were collected at 100K temperature on a Bruker APEX(II) DUO CCD diffractometer using Mo $K_\alpha$ radiation (λ = 0.71073 Å), $\omega$-scans ($2\theta$ = 57.14), for a total of 15677 independent reflections. Space group P 21, a = 11.261(3), b = 20.461(5), c = 14.368(4), $\gamma$=108.903(6),V = 3132.1(14)Å$^3$, monoclinic, Z = 2 for chemical formula $C_{47}$ $H_{85}$ $Cl_3$ $N_6$ $O_{13}$, with one molecule in asymmetric unit; $\rho$calcd = 1.112gcm$^{-3}$, $\mu$ = 0.202mm$^{-1}$, F(000) = 4599, The structure was obtained by direct methods using SHELXS-97.[1] The final R value was 0.1173 (wR2 = 0.0.2310) 6854 observed reflections ($F_0 \geq 4\sigma(|F_0|)$) and 637variables, S = 1.212.The largest difference peak and hole were 0.846and -0.436Å$^3$, respectively

**Acknowledgements**

R. M is thankful to CSIR for fellowship. HNG thank IISER-Pune for financial support.

**Keywords:** achiral peptides • foldamers • tendril perversion • $3_{10}$-helix • Schellman motif

## REFERENCES

[1] a) P. Cintas, *Angew. Chem. Int. Ed.* **2002**, *41*, 1139–1145; b) M. Rickhaus, M. Mayor. M. Juríček, *Chem. Soc. Rev.,* **2016**, *45*, 1542-1556; d) Y. Wang, J. Xu, Y. Wang, H. Chen, *Chem. Soc. Rev*., **2013**, *42*, 2930–2962.

[2] M. Novotny, G. J. Kleywegt, *J. Mol. Biol.*, **2005**, *347*, 231–241.

[3] a) S. Aravinda, N. Shamala, P. Balaram, *Chem. Biodiversity,* **2008**, *5*, 1238-1262; b) J. Venkatraman, S. C. Shankaramma, P. Balaram, *Chem. Rev*., **2001**, *101*, 3131-3152; c) I. L. Karle, P. Balaram, *Biochemistry,* **1990**, *29*, 6747-6756; d) C. Toniolo, M. Crisma, F. Formaggio, C. Peggion, Biopolymers, **2001**, *60*, 396-419; e) B. A. F. LeBailly, J. Clayden, *Chem. Commun*., **2016**, *52*, 4852-4863; f) M. Crisma, M. De Zotti, F. Formaggio, C. Peggion, A. Moretto, C. Toniolo, *J. Pept. Sci*., **2015**, *21*, 148–177.

[4] a) J. Clayden, A. Castellanos, J. Solá, G. A. Morris, *Angew. Chem. Int. Ed.*, **2009**, *48*, 5962-5965; b) J. Solá, G. A. Morris, J. Clayden, *J. Am. Chem. Soc.*, **2011**, *133*, 3712 – 3715; c) J. Solà, M. Helliwell, J. Clayden, *Biopolymers*, **2011**, *95*, 62-69; d) R. A. Brown, T. Marcelli, M. De Poli, J. Solá, J. Clayden, *Angew. Chem., Int. Ed*., **2012**, *51*, 1395–1399; e) T. Boddaert, J. Solá, M. Helliwell, J. Clayden, *Chem. Commun*., **2012**, *48*, 3397–3399; f) J. Solá, M. Helliwell, J. Clayden, *J. Am. Chem. Soc*., **2010**, *132*, 4548–4549.

[5] a) D. Seebach, A. K. Beck, D. J. Bierbaum, *Chem. Biodiversity* **2004**, *1*, 111-1239; b) W. S. Horne, S. H. Gellman, *Acc. Chem. Res.,* **2008**, *41*, 1399-1408; c) R. P. Cheng, S. H. Gellman, W. F. DeGrado, *Chem. Rev.,* **2001**, *101*, 3219-3232; d) F. Fülöp, T. A. Martinek, G. K. Tóth, *Chem. Soc. Rev.,* **2006**, *35*, 323-334; e) G. Guichard, I. Huc, *Chem. Commun.,* **2011**, *47*, 5933-594; f) P. G. Vasudev, S. Chatterjee, N. Shamala, P. Balaram, *Chem. Rev.,* **2011**, *111*, 657-687; g) T. A. Martinek, F. Fülöp, *Chem. Soc. Rev.*, **2012**, *41*, 687-702; h) F. Bouillère, S. Thétiot-Laurent, C. Kouklovsky, V. Alezra, *Amino Acids,* **2011**, *41*, 687-707.

[6] a) S. Shin, M. Lee, I. A. Guzei, Y. K. Kang, S. H. Choi, *J. Am. Chem. Soc.,* **2016**, *138*, 13390-13395; b) K. Basuroy, B. Dinesh, M. B. M. Reddy, S. Chandrappa, S. Raghothama, N. Shamala, P. Balaram, *Org. Lett*., **2013**, *15* , 4866–4869.

[7] S. Abele, P. Seiler, D. Seebach, *Helv. Chim. Acta*, **1999**, *82*, 1559–1571.

[8] D. Seebach, T. Sifferlen, D. J. Bierbaum, M. Rueping, B. Jaun, B. Schweizer, J. Schaefer, A. K. Mehta, R. D. O' Connor, B. H. Meier, M. Ernst, A. Glättli, *Helv. Chim. Acta*, **2002**, *85*, 2877 -2917.

[9] P. G. Vasudev, N. Shamala, K. Ananda, P. Balaram, *Angew. Chem. Int. Ed*., **2005**, *44*, 4972–4975.

[10] S. Chatterjee, P. G. Vasudev, S. Ragothama, C. Ramakrishna, N. Shamala, P. Balaram, *J. Am. Chem. Soc.,* **2009**, *131*, 5956- 5965.

[11] S. V. Jadhav, H. N. Gopi, *Chem. Commun*., **2013**, *49*, 9179-9181.

[12] R. Misra, A. Saseendran, G. George, K. Veeresh, K. M. P. Raja, S. Raghothama, H.-J Hofmann, H. N. Gopi, *Chem. Eur. J* **2017**, *23*, 3764.

[13] M. G. Kumar, S. M. Mali, H. N. Gopi, *Org. Biomol. Chem.,* **2013**, *11*, 803–813.

[14] A. Goriely, M. Tabor, *Phys. Rev. Lett.,* **1998**, *80*, 1564–1567.

[15] M. Tomsett, I. Maffucci, B. A. F. Le Bailly, L. Byrne, S. M. Bijvoets, M. G. Lizio, J. Raftery, C. P. Butts, S. J. Webb, A. Contini, J. Clayden, *Chem. Sci*., **2017**, *8*, 3007-3018.

[16] A. Banerjee, S. Raghothama, I. L. Karle, P. Balaram *Biopolymers,* **1996**, *39*, 279–285.

[17] a) C. Baldauf, R. Günther H.-J. Hofmann, *J. Org. Chem.,* **2006**, *71*, 1200-1208; b) C. Baldauf, R. Genther, H.-J. Hofmann, Biopolymers 2005, 80, 675; c) S. V. Jadhav, A. Bandyopadhyay, H. N. Gopi, *Org. Biomol. Chem*., **2013**, *11*, 509-514; d) B. F. Fisher, S. H. Gellman, *J. Am. Chem. Soc.*, **2016**, *138*, 10766-10769. e) C. Bonnel, B. Legrand, M. Simon, J. Martinez, J.-L. Bantignies, Y.K. Kang, E. Wenger, F. Hoh, N. Masurier, L. T. Maillard, *Chem. Eur. J*. **2017**, *23*, 17584 – 17591.f) S. Shankar, N. A. Wani, U. P. Singh, R. Rai *ChemistrySelect,* **2016**, *1*, 3675 – 3678

[18] Schellman, In *Protein Folding;* Jaenicke, R., Ed.; Elsevier/North-Holland Biochemical Press: Amsterdam, **1980**, 53-61.

[19] a) S. Aravinda, N. Shamala, A. Bandyopadhyay, P. Balaram *J. Am. Chem. Soc.*, **2003**, *125*, 15065–15075; b) S. J. Pike, J. Raftery, S. J. Webb, J. Clayden, *Org. Biomol. Chem*., **2014**, *12*, 4124-4131; c) N. Ousaka, Y. Inai *J. Am. Chem. Soc*., **2006**, *128*, 14736–14737; d) N. E. Shepherd, H. N. Hoang, G. Abbenante, D. P. Fairlie *J. Am. Chem. Soc.*, **2009**, *131*, 15877–15886; e) V. Maurizot, C. Dolain, Y. Leydet, J. M. Léger, P. Guionneau, I. Huc *J. Am. Chem. Soc.,* **2004,** *126*, 10049–10052; f) S. Aravinda, N. Shamala, A. Pramanik, C. Das, P. Balaram *Biochem. Biophys. Res.*

10.1002/asia.201901411

*Commun*., *273*, 933–936; g) I. L. Karle *Biopolymers peptide science*. **2001,** *60*, 351–365; h) A. Banerjee, S. Raghothama, I. L. Karle, P. Balaram *Biopolymers*, **1996**, *39*, 279–285; i) S. Datta, N. Shamala, A. Banerjee, A. Pramanik, S. Bhattacharjya, P. Balaram *J. Am. Chem. Soc*., **1997**, *119*, 9246-9251. j) S.-I, Sakurai, S. Ohsawa, K. Nagai, K. Okoshi, J. Kumaki, E, Yashima, *Angew. Chem. Int. Ed*. **2007**, *46*, 7605 – 7608. k) S, Lifson, C. E. Felder, M. M. Green, *Macromolecules* **1992**, *25*, 4142-4148.

10.1002/asia.201901411

## Table of Contents

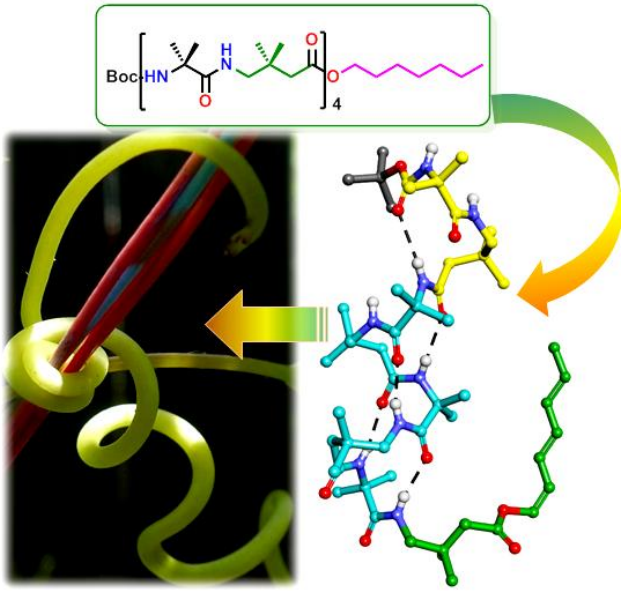


We are reporting the co-existence of left- and right-handed helical screw sense along with the C-terminal helix terminating property within the single molecule of new achiral α,γ-hybrid peptide foldamers. The molecular level left- and right–handed helix conformation representing the macroscopic tendril perversion